J Mol Model (2010) 16:1047–1058
DOI 10.1007/s00894-009-0618-7

ORIGINAL PAPER

Docking of sialic acid analogues against influenza A hemagglutinin: a correlational study between experimentally measured and computationally estimated affinities

Mohammed Noor Al-qattan · Mohd Nizam Mordi

Received: 5 August 2009 / Accepted: 21 October 2009 / Published online: 13 November 2009

Abstract A molecular docking tool of AutoDock3.05 was evaluated for its ability to reproduce experimentally determined affinities of various sialic acid analogues toward hemagglutinin of influenza A virus. With the exception of those with a C6-modified glycerol side chain, the experimental binding affinities of most sialic acid analogues (C2, C4 and C5-substituted) determined by viral hemadsorption inhibition assay, hemagglutination inhibition assay and nuclear magnetic resonance correlated well with the computationally estimated free energy of binding. Sialic acid analogues with modified glycerol side chains showed only poor correlation between the experimentally determined hemagglutinin inhibitor affinities and AutoDock3.05 scores, suggesting high mobility of the glutamic acid side chain at the glycerol binding pocket, which is difficult to simulate using a flexi-rigid molecular docking approach. In conclusion, except for some glycerol-substituted sialic acid analogues, the results showed the effectiveness of AutoDock3.05 searching and scoring functions in estimating affinities of sialic acid analogues toward influenza A hemagglutinin, making it a reliable tool for screening a database of virtually designed sialic acid analogues for hemagglutinin inhibitors.

Keywords Hemagglutinin · Sialic acid analogues · Molecular docking · Affinity

Introduction

Influenza A virus—an enveloped negative strand RNA virus belonging to the *Orthomyxoviridae* family—is responsible for annual influenza epidemics and recurrent pandemics. There are many serotypes of influenza A, which are classified by the antigenicity of their corresponding surface glycoproteins hemagglutinin (HA) and neuraminidase (NA) [1, 2]. HA is responsible for sticking the virus to the host cell surface-bound sialic acid (SA) moieties followed by endocytosis [3]. NA is responsible for releasing progeny virus from the infected cell by hydrolysing O-glycosidic bonds between the terminal SA, which is bound to HA, and the penultimate sugar moiety that connects SA to the host cell membrane [4]. As the functions of HA and NA oppose each other, a balancing act is required for effective viral infection [5]. HA and NA are highly vulnerable to mutagenic change by shift and/or drift in response to the pressure of the host immune system, explaining why vaccination against influenza A virus is ineffective and pandemics are recurrent.

SA (5-amino-3,5-dideoxy-D-glycero-D-galacto nonurosonic acid) is a member of the natural sialic acids family and is the natural ligand of both of HA and NA [6]. A pyranose ring forms the scaffold of the SA molecule, to which different functional groups are connected through carbon atoms C2, C4, C5 and C6. Natural SA has been modified to produce monovalent inhibitors, and incorporating several molecules of low affinity SA analogues onto large molecular weight carriers could lead to polyvalent inhibitors [7, 8].

Thus far, no effective HA inhibitor has been designed, which could be attributed to the low affinity between many SA analogues and the shallow binding site of HA. Due to the current pandemic of H1N1, and the possibility of H5N1 resurgence, and the resistance that has developed to current treatment [9], HA, which presents on the viral surface as a homotrimer, can be used as an alternative target to combat influenza A virus. Each monomer has a primary binding site located at HA1, and a secondary binding site located at

M. N. Al-qattan · M. N. Mordi (✉)
Centre for Drug Research, Universiti Sains Malaysia,
11800 Minden, Penang, Malaysia
e-mail: mnizam@usm.my

the interface between HA1 and HA2. Various SA analogues bound to HA have been studied using X-ray crystallography, and many of these analogues have been shown to bind HA1 at approximately the same crystal position [10, 11]. The availability of three-dimensional structures of HA co-crystallized with various inhibitors provides a good basis for using structure-based techniques for the discovery of new inhibitors.

Although docking and scoring methods have been used intensively in the estimation of the affinity of various drug-like compounds against their molecular target, no docking study has yet evaluated experimental binding affinities of SA analogues against HA. As the inhibitory potency of SA analogues has been well documented using various techniques such as nuclear magnetic resonance (NMR) [11–14], viral hemadsorption inhibition assays [15, 16] and viral hemagglutination inhibition assays [17], we aim to study the effectiveness of AutoDock3.05 in correlating these experimental affinities with computationally estimated free energy of binding of SA analogues, which could be implemented in the design of new virtual SA compounds [18]. In this paper, AutoDock3.05 was selected as the docking program since the SA–HA complex was one of the ligand–protein complexes that was included in the training set used to derive energy coefficients for the AutoDock3.05 semi-empirical scoring function [19].

Methods

Preparation of protein structure

The HA crystal structure of influenza A H3N2 (X-31) virus with methyl-α-Neu5Ac (PDB ID 1HGH) is composed of six domains (three HA1 and three HA2). All ligands that bind to the primary and secondary binding sites were removed as well as all water molecules. Based on the crystallographic structure of HA in complex with methyl-alpha-neuraminic acid (PDB ID 1HGH) and with other SA analogues [10, 11], no conserved water molecules are visible near the primary binding pocket and consequently thought to participate in the intermolecular interaction between the HA and ligands. Therefore, as the docking experiments were carried out specifically against the primary binding site, all water molecules observed in the crystal structure were removed (whether close to primary or secondary binding sites) before Kollman charge was assigned.

The structure was checked for any missing or erroneous side chains using DeepView / Swiss-PdbViewer v3.7 software (http://www.expasy.org/spdbv/). Using AutoDockTools 1.4.5, hydrogen atoms were added to the protein. The protonation state of His183, which forms a hydrogen-bond network with residues Tyr98, Tyr195, and Trp153 [10, 11], was corrected, whereby the hydrogen was assigned to the nitrogen atom at the epsilon position (Fig. 1). Kollman united-atom charges, fragmental volumes, and desolvation parameters were subsequently assigned.

Preparation of SA analogue molecular structures

Molecular structures of SA analogues and their corresponding experimental affinities toward H3N2 (X-31) HA were retrieved from the literature and divided into three groups. Group 1 comprised analogues with relative IC_{50} values observed through competitive hemadsorption inhibition assays [15, 16]. Group 2 comprised analogues of large C2-substitutions with relative affinities determined by hemagglutination inhibition assays [17], while group 3 comprised analogues with dissociation constants determined by NMR experiments [11–13]. The three-dimensional (3D) structures of SA analogues were constructed using HyperChem 6.01 and subjected to geometry optimization by

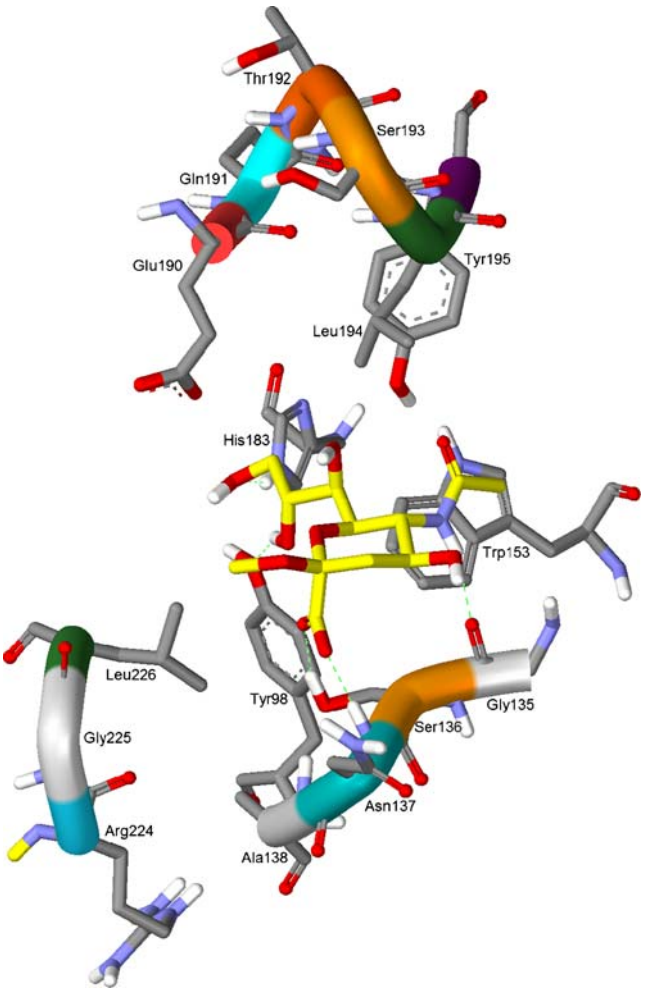

Fig. 1 Binding of sialic acid (SA; *yellow*) against the hemagglutinin 1 (HA1) binding pocket of influenza A virus H3N2 (X-31). *Dashed green lines* Intermolecular hydrogen (H)-bonds

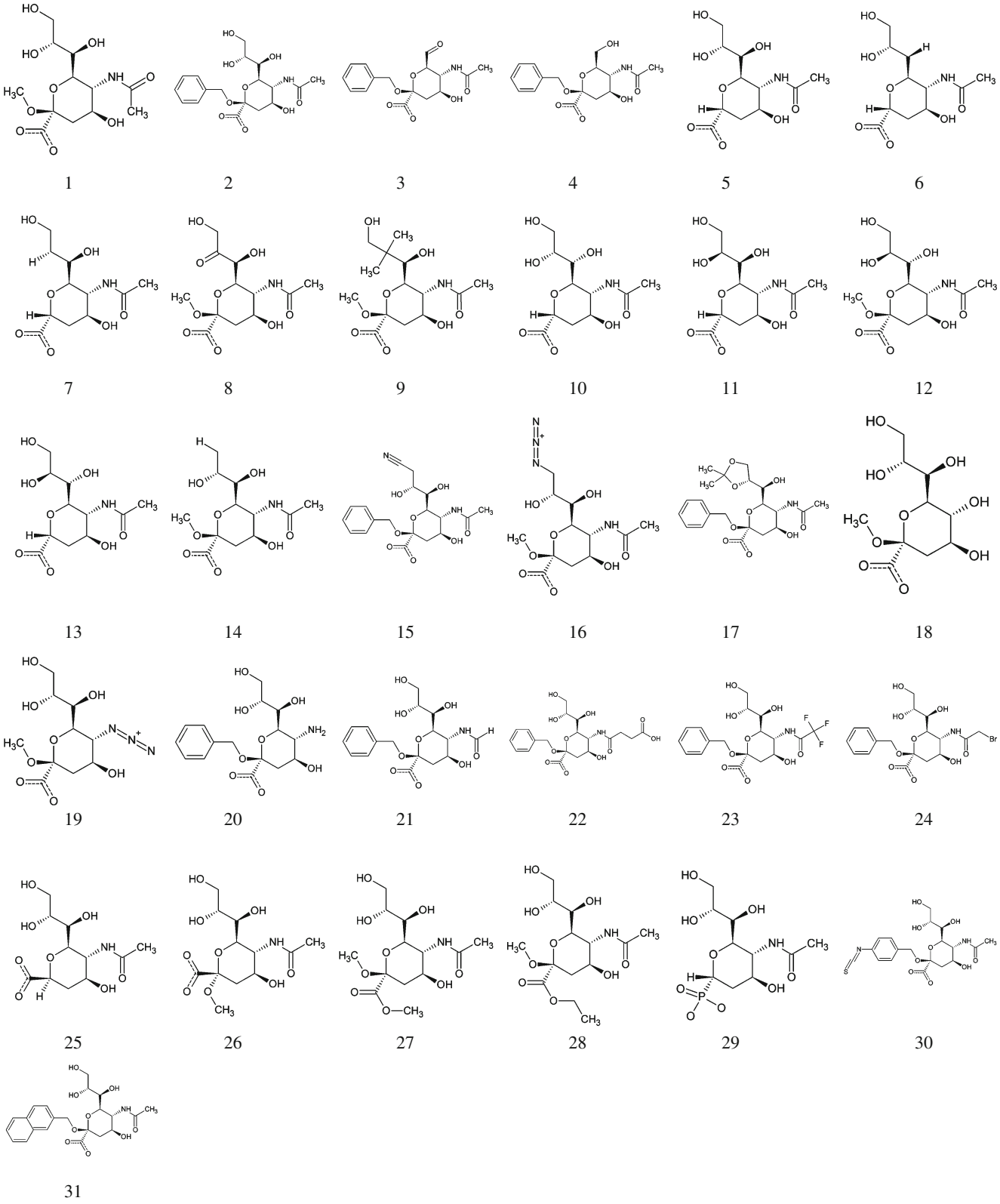

Scheme 1 Group 1 sialic acid (SA) analogues, in which IC_{50} values were derived from hemadsorption inhibition assay [15, 16]

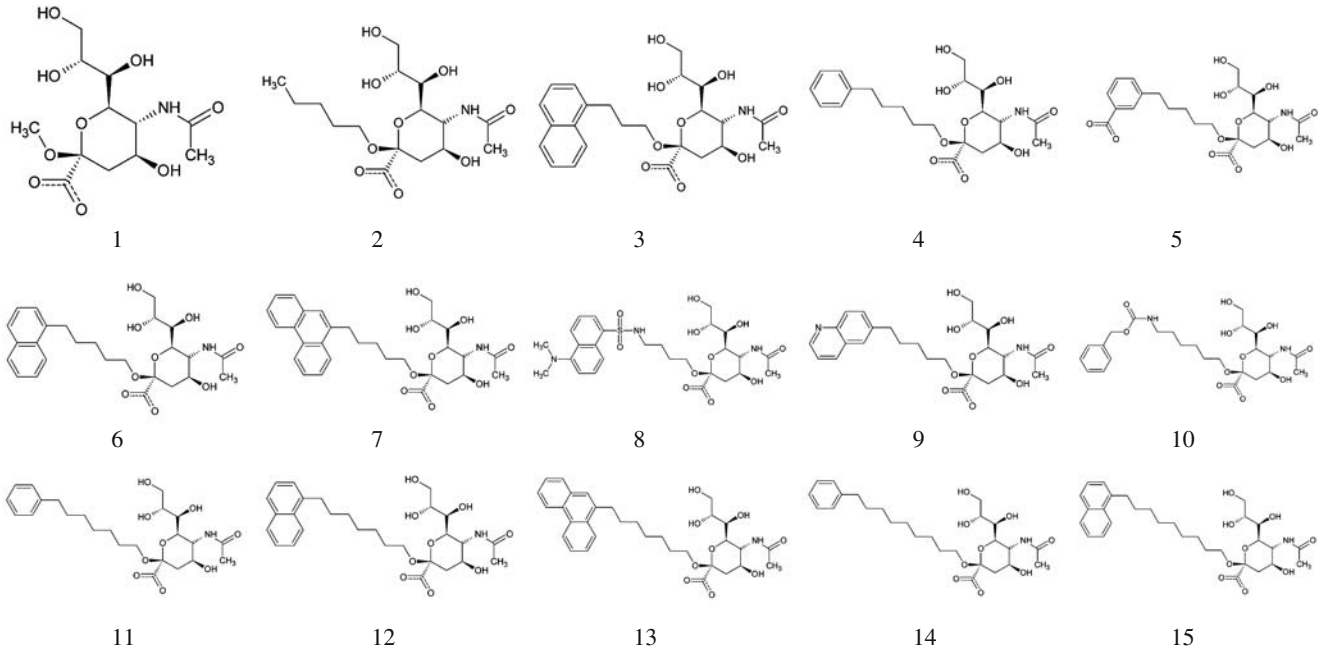

Scheme 2 Group 2 SA analogues, in which relative affinities were calculated from hemagglutination inhibition assay [17]

Steepest Descent followed by Polak Ribiere methods using MM+ force field. The positions and orientations of the generated molecules in space were superimposed on that of crystal methyl-α-Neu5Ac using the pyranose rings of the ligand. Gasteiger charges were added to the ligand atoms using VEGA ZZ 2.0.8 (http://www.vegazz.net/) software. Autotors (an AutoDock utility) was used to define the rotatable bonds within the ligand, if any, and unite the

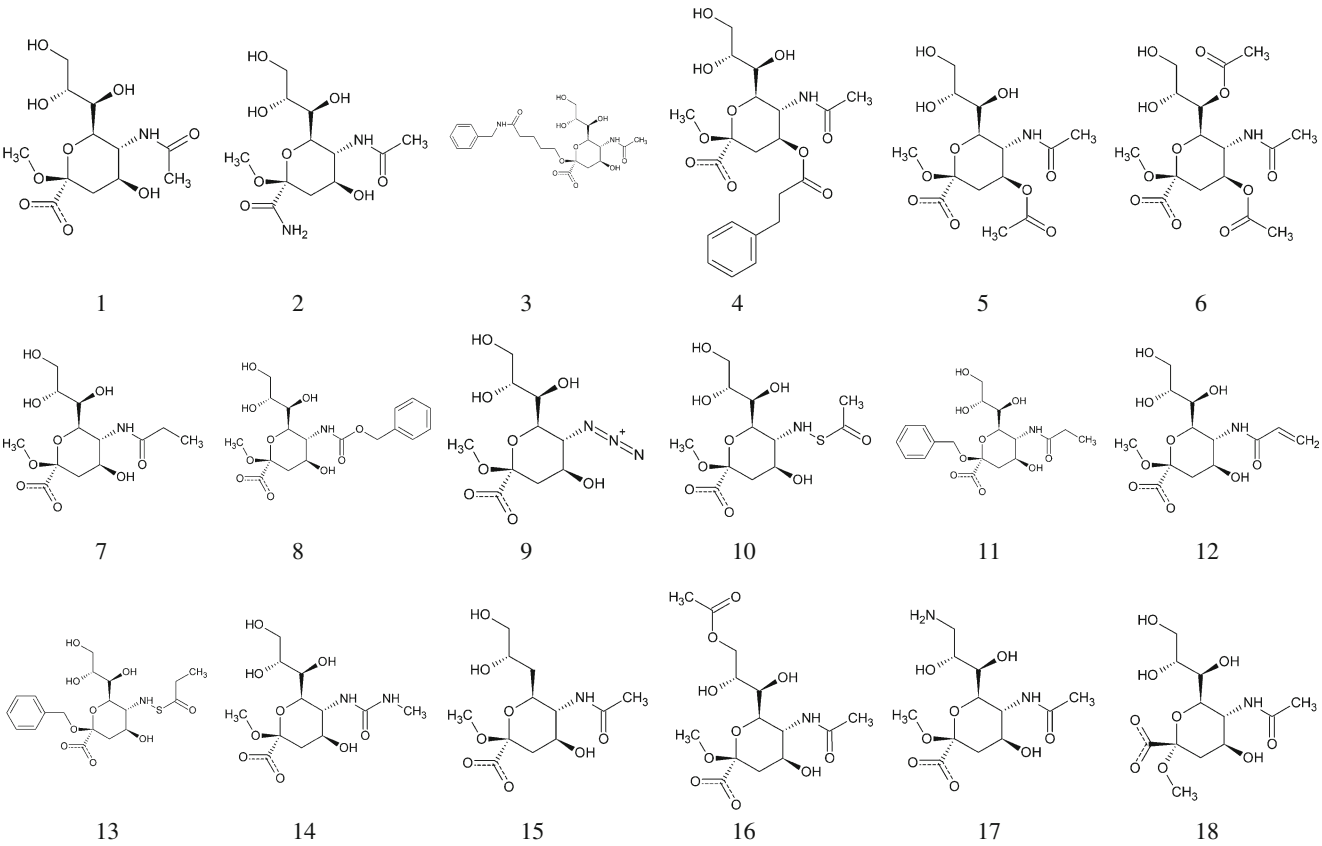

Scheme 3 Group 3 SA analogues, in which dissociation constants were calculated by nuclear magnetic resonance (NMR) experiments [11–13]

charges of nonpolar hydrogens with the carbon atoms bearing them.

Assigning docking parameters

The grid box used to calculate the pairwise atomic interaction maps between ligand and protein atoms was manually centered on the HA1 binding pocket without using any specific atom as a central reference point. Automatic grid box positioning was not used because of the large variation in the size of the docked compounds, especially for C2-derived analogues (Group 2 compounds). The grid box was adjusted to be large enough to cover all the amino acids that form the natural SA binding site in addition to those at the boundary. The grid box (X, Y, Z dimension) for Group 2 compounds is 77, 85 and 41 points, while the remaining compounds used a grid box of 70, 40 and 50 points. The spacing between grid points in each dimension was 0.375 Å.

Since large conformational space was available (due to a large number of ligand rotatable bonds, i.e., between 7 and 22), the parameters of the Lamarckian Genetic Algorithm (LGA) were selected to enable an exhaustive conformational search. As Autodock3.05 enables flexible-rigid docking, the conformational space of the compounds can be explored on using LGA during docking simulation. LGA is a combination of a genetic algorithm and a local search that is capable of

Table 1 Computational values of group 1 sialic acid (SA) analogues. *EFEB* AutoDock3.5 estimated free energies of binding, K_i inhibitory constants, *RMSD* calculated root mean squares deviation of the pyranose ring in relation to the crystal methyl-α-Neu5Ac. The observed values represent relative affinities (RA)

Analogue no.	Computational values			Observed values	
	EFEB (kcal/mol)	K_i (mol)	RMSD of pyranose Å	RA	−log(RA)
Group 1-A: SA analogues with modification in the glycerol side chain					
1	−4.34	6.62E-04	0.52	1	0.00
2	−4.71	3.50E-04	0.68	1	0.00
3	−4.90	2.56E-04	0.78	0.08 [a]	1.10
4	−4.73	3.41E-04	0.80	0.1	1.00
5	−4.70	3.60E-04	0.45	0.67	0.17
6	−5.11	1.80E-04	0.68	0.09 [a]	1.05
7	−4.76	3.24E-04	0.66	0.18	0.74
8	−4.51	4.96E-04	0.75	0.14 [a]	0.85
9	−4.64	3.98E-04	0.54	0.14 [a]	0.85
10	−3.93	1.32E-03	0.67	0.06	1.22
11	−4.53	4.79E-04	0.66	0.19	0.72
12	−3.64	2.16E-03	0.49	0.21	0.68
13	−4.00	1.17E-03	0.51	0.16	0.80
14	−4.40	5.96E-04	0.68	1	0.00
15	−5.31	1.27E-04	0.68	0.17 [a]	0.77
16	−4.58	4.43E-04	0.72	0.11 [b]	0.96
17	−5.22	1.50E-04	4.11	0.2	0.70
Group 1-B: SA analogues with modification in the N-acetyl group					
18	−3.28	3.96E-03	0.75	0.07 [a]	1.15
19	−3.58	2.39E-03	0.74	0.07 [a]	1.15
20	−4.13	9.32E-04	5.08	0.36 [b]	0.44
21	−4.27	7.38E-04	0.68	0.34 [b]	0.47
22	−4.12	9.56E-04	1.83	0.34 [a]	0.47
23	−4.72	3.45E-04	0.67	0.34 [a]	0.47
24	−5.03	2.04E-04	0.66	0.34 [b]	0.47
Group 1-C: SA analogues with modifications of the substituents at C2					
25	−4.06	1.06E-03	3.21	0.067 [b]	1.17
26	−3.62	2.23E-03	1.82	0.001 [a]	3.00
27	−3.57	2.43E-03	0.86	0.1 [a]	1.00
28	−3.87	1.45E-03	0.92	0.1 [a]	1.00
29	−4.83	2.89E-04	0.52	0.13	0.89
30	−5.06	1.95E-04	0.35	2	−0.30
31	−5.49	9.53E-05	0.60	1.2	−0.08

[a] Inhibition potency was below 50% at highest concentration tested

[b] No inhibition was observed

exploring the flexibility of the compounds in order to find the lowest bound energy conformation. Initial translation, quaternion and torsions, which determine the initial ligand position, orientation, and conformation, were taken to be random (except for docking the large SA analogues of group 2, they were kept in minimized form to avoid exhaustive sampling of improbable conformational space). The translation step was 1 Å, and quaternion and torsion steps were 50 degrees. In LGA, the number of population individuals was 150, the maximum number of evaluations that LGA should make within a single run was 2.5 million, and the maximum number of generations was 27,000. Pseudo-Solis and Wets algorithm was used for local search with application frequency equal to 0.09. One hundred LGA runs were performed, and docked conformations of the relative root mean square deviation (RMSD) were clustered together within a tolerance of 2 Å. Default values were assigned for the remaining docking parameters.

Correlation between observed and estimated affinities

The correlation between observed and estimated affinities of SA analogues toward HA1 of influenza A H3N2 (X-31) was calculated in order to evaluate the reliability of the molecular docking technique in differentiating between active and inactive analogues. Regression analysis using Unscrambler 9.7 software (Camo ASA) was used to provide the correlations, and was measured by the value of the correlation coefficient (r). Throughout the course of the correlation, the observed affinities were expressed using either of two expressions of relative affinities (RA; Group 1 and Group 2 analogues) or observed free energy of binding (OFEB; Group 3 analogues). The RA of a given analogue equals the ratio of the IC_{50} value of a reference SA analogue (usually methyl-α-Neu5Ac) to the IC_{50} value of that particular analogue. Values of OFEB were obtained by applying the classical Arrhenius equation [OFEB = (ln K_d) × R_{cal} × T_k] to the experimental dissociation constants (K_d), where R_{cal} is the gas constant, i.e., 1.98719 cal K^{-1} mol^{-1}, and T_k is the temperature in Kelvin, i.e., 298.15 K.

Results

The molecular structures of SA analogues in groups 1, 2, and 3 are shown in Schemes 1, 2 and 3, respectively. For each studied SA analogue, the estimated free energy of binding (EFEB), inhibitory constant (K_i), and RMSD of the pyranose ring of the pyranose of crystal methyl-α-Neu5Ac were calculated. The RMSD value indicates the effect of the structural modification on the analogue's positional shiftage from the crystal SA binding site.

The docking results obtained from docking group 1 against the HA1 binding pocket together with the reported experimental values are summarized in Table 1. The docking results showed that, with the exception of analogues 17, 20, 25, and 26, all SA analogues bound HA1 with conformations comparable to that of the crystal methyl-α-Neu5Ac conformation. The correlation between EFEB −log(RA) values was established using linear regression analysis (Fig. 2). Linear regression analysis with r^2 values has previously been used to correlate experimental and calculated affinities [20–23]. The correlation coefficient (r) of 0.45 obtained for group 1 analogues suggests a weak correlation between estimated and observed affinities [22, 23]. In order to identify the cause of the low r value for group 1, the group was subdivided further into group 1-A, -B, and -C according to whether the modification encompassed the glycerol chain, N-acetyl, or C2-substituent, respectively. A separated 2D scatter plot was then constructed for each of the three constitutive sub-groups.

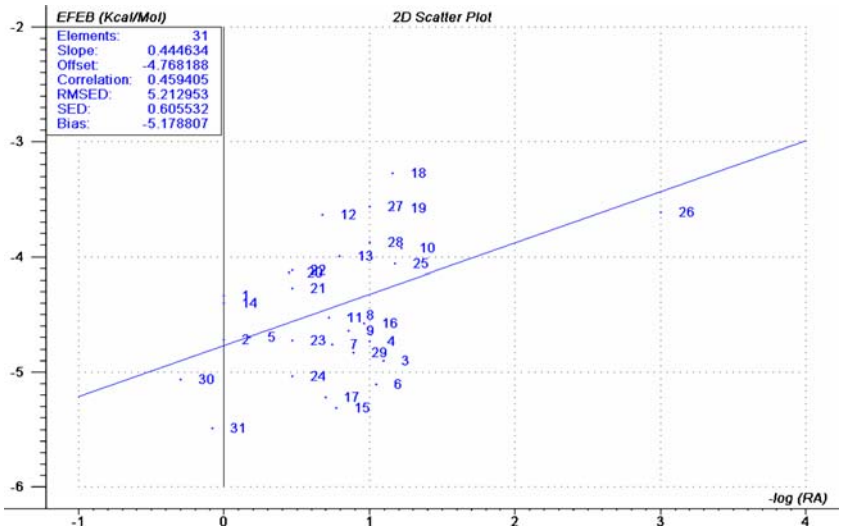

Fig. 2 Regression analysis showing the correlation between the value of estimated free energy of binding (EFEB) calculated by AutoDock3.05 and the negative logarithmic value of the experimentally determined relative affinity ([−log (RA)] for group 1 SA analogues. Individual values are listed in Table 1

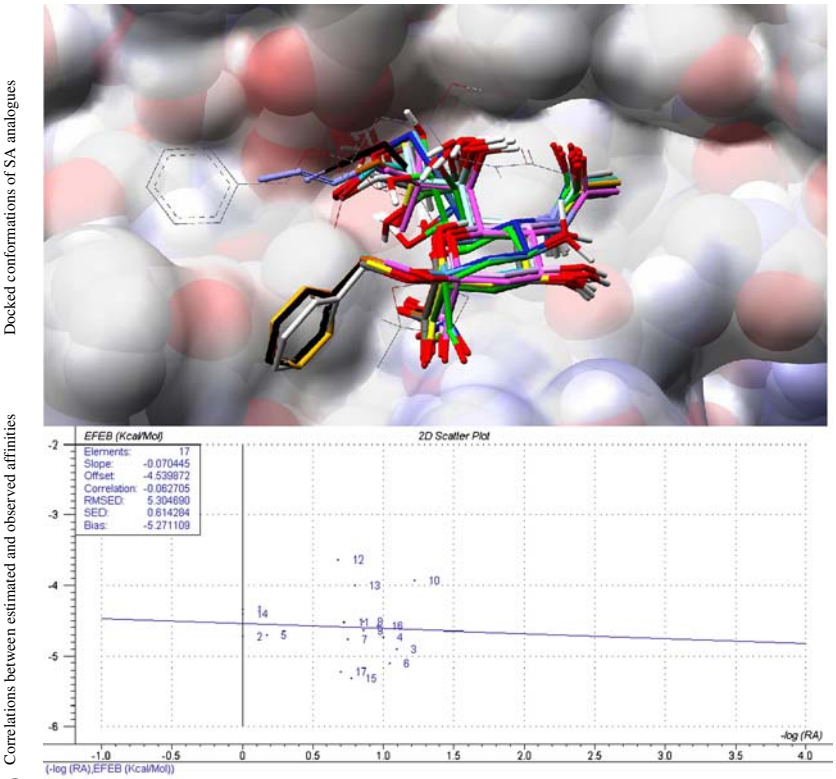

a SA analogues of modified glycerol side chain

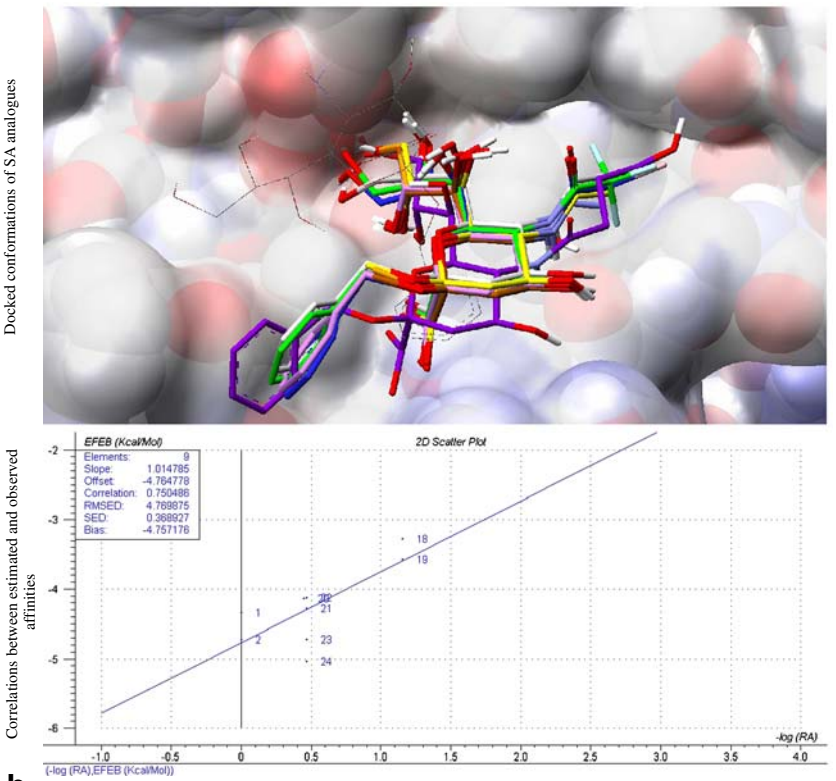

b SA analogues of modified N-acetyl group

Fig. 3 a–c Upper panels Docked conformations of SA analogues. Lower panels 2D-scatter plots showing the correlation between the EFEB value calculated by AutoDock3.05 and −log (RA) for SA analogues. **a** Group 1-A, **b** group 1-B, **c** group 1-C

Fig. 3 (continued)

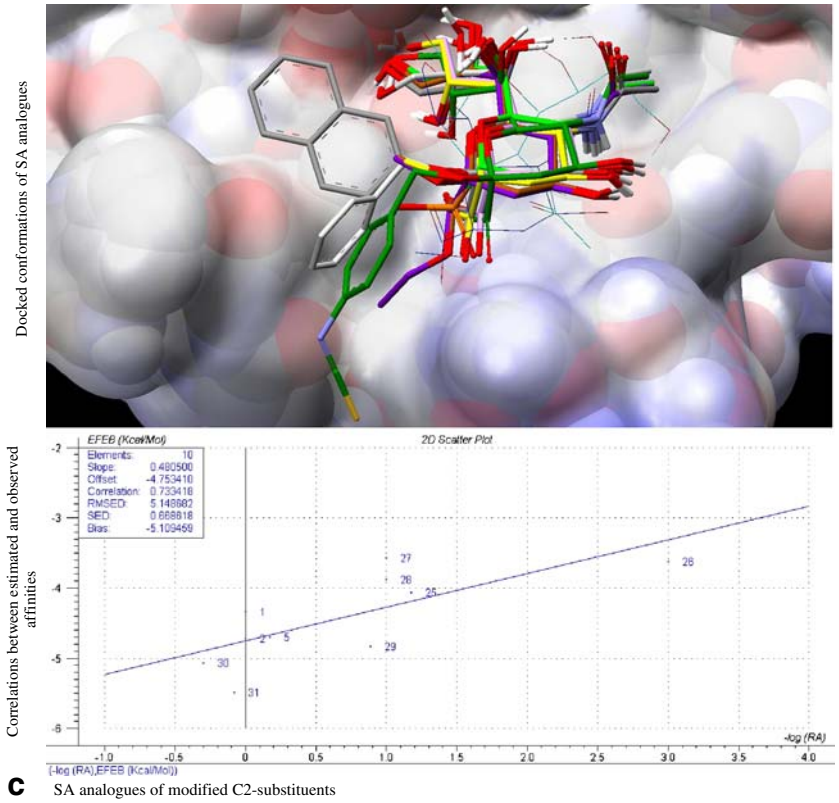

Values of EFEB correlated well with the −log(RA) for SA analogues with a modified N-acetyl group (r=0.75, Fig. 3b) and modified C2-substituents (r=0.73, Fig. 3c). On the other hand, poor correlation was obtained for SA analogues with a modified glycerol side chain (r=−0.06, Fig. 3a), which can be attributed to the unexpectedly low values of EFEB calculated for some SA analogues that are experimentally inactive (e.g., analogues 3, 6, 15, and 17).

On the other hand, all SA analogues of group 2 bound HA1 with conformations comparable to that of the crystal methyl-α-Neu5Ac conformation (Fig. 4b). These analogues possess different substitutions connected to pyranose carbon C2 via molecular linkers of different lengths. According to molecular docking simulations, large linkers allow the connected substitutions to flip between either of the two nearby structural grooves (grooves A and B). The binding improvements in this group of SA analogues were mediated mainly by hydrophobic interactions to either of the two grooves. Better correlation between EFEB and −log(RA) was obtained for group 2, for which r = 0.78 (Table 2, Fig. 4a).

Group 3 comprises SA analogues with different modifications of the glycerol side-chain, N-acetyl group, C2-substituents, and at the C4-hydroxyl. These analogues bound to HA1 with conformations comparable to that of the crystal methyl-α-Neu5Ac conformation (Fig. 5b). The docking results together with the experimental values are provided in Table 3. A correlation coefficient of 0.79 was obtained between the observed free energy of binding (OFEB) and the EFEB (Fig. 5a) suggesting an acceptable correlation between experimental and calculated affinities [20–23].

Discussion

The EFEB values calculated by AutoDock3.05 correlated well with the observed affinities for SA analogues of group 2 (r=0.78) and group 3 (r=0.79) SA analogues. With respect to group 1 analogues, the correlation coefficient of 0.46 suggests a poorer correlation between experimental and calculated affinities. As group 1 comprised analogues with different C2, C5 and C6 side chains, the analogues were subdivided further according to their side chains in order to determine the cause of the poorer correlation value (group 1-A = modified glycerol side chain, group 1-B = modified N-acetyl group and group 1-C = modified C2-substituents). Values between EFEB and experimental affinities for group 1B and 1C inhibitors were well correlated, suggesting the scoring reliability of the software. The correlation coefficients and standard error values are comparable to other studies [22]. On the other hand, poor correlation was obtained for group 1-A (modified glycerol side chain), with correlation coefficient and standard error values of −0.06 and 0.61, respectively. It is interesting that

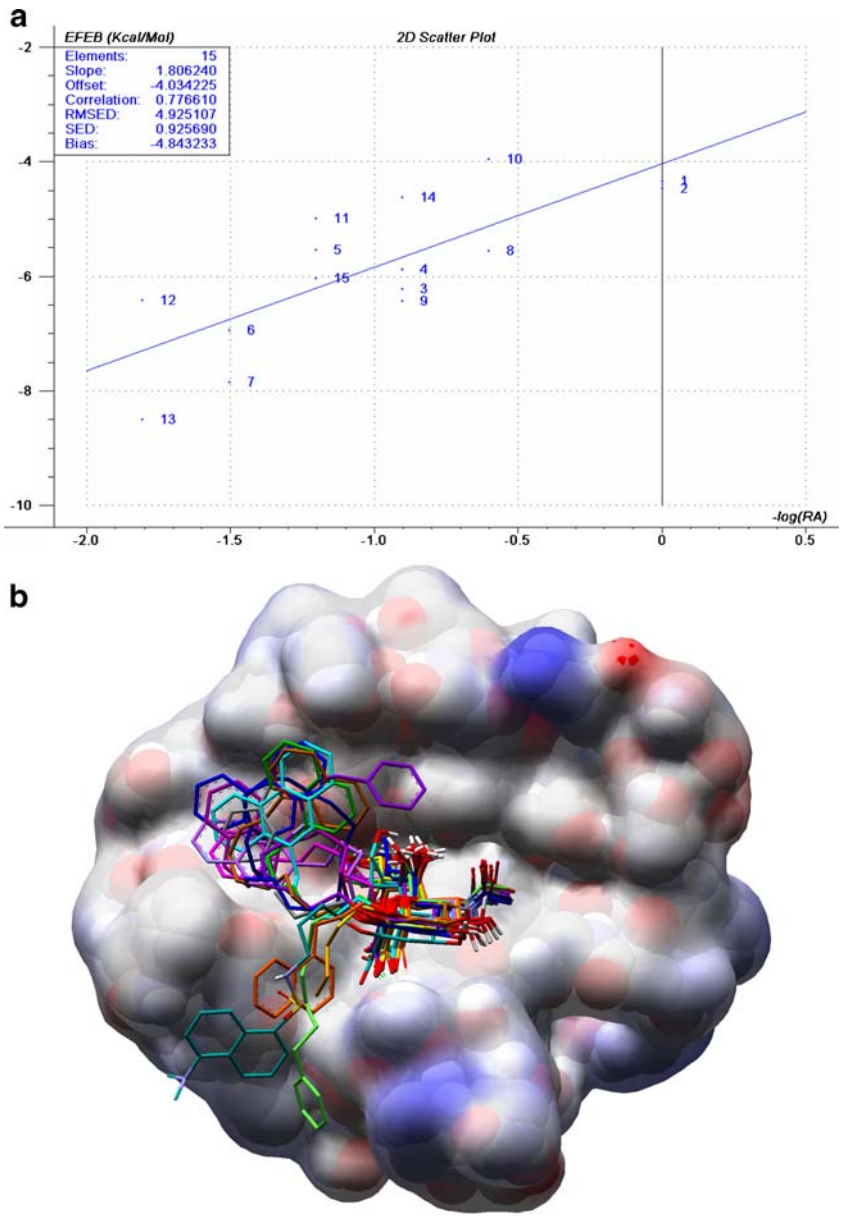

Fig. 4 a,b Docking results for group 2 SA analogues. **a** Regression analysis showing the correlation between the EFEB value calculated by AutoDock3.05 and −log (RA) for all SA analogues listed in Table 2. **b** The docked conformations of SA analogues show that C2-substitutions extend to either of two nearby grooves

these inhibitors have such low scores. One might speculate that this may be attributed to the high temperature factor (mobility) of the amino acid side chains (mainly Glu190) that form the glycerol binding site [11, 24]. As mobility of the receptor protein is necessary to accommodate ligands and was totally omitted in the AutoDock3.05 flexible-rigid docking procedure, inaccurate binding energies may be calculated for some SA analogues with modified glycerol side chains.

An attempt to investigate this possibility was carried out using another docking study with AutoDock4.0.1, which allows for flexibility in the receptor side chains. Similar to the previous experiment, the ligand molecules were set as flexible. With respect to HA, three residues (Thr 155, Leu 194, Glu 190) were selected as flexible residues in Autodock 4 simulations since correspond to some of the amino acids in the binding pocket. Furthermore, Leu194 and Glu190 interact directly with the C6-glycerol side chain of SA while Thr155 is closed to the C5-N-acetyl side chain. However, the AutoDock4.0.1 approach of both flexible-flexible and flexible-rigid docking algorithms failed to reproduce even the crystal conformation of methyl-α-Neu5Ac (data not shown), which may be attributed to the modifications introduced to the AutoDock4.0.1 scoring function [25]. Other researchers have reported that inexact linearity could exist between $-\log(IC_{50})$ or −log(RA) and energy [26]; however, in our study only group 1 analogues showed this characteristic and not group 2 inhibitors, suggesting compound selection is more important than the type of affinity values used to construct the

Table 2 Computational values for group 2 SA analogues. Definitions as in Table 1

Analogue no.	Computational values			Observed values	
	EFEB (kcal/mol)	K_i (mol)	RMSD of pyranose Å	RA	−log(RA)
1	−4.33	6.62E-04	0.52	1.00	0.00
2	−4.46	5.38E-04	0.54	1.00	0.00
3	−6.22	2.76E-05	0.72	8.00	−0.90
4	−5.88	4.91E-05	0.68	8.00	−0.90
5	−5.54	8.68E-05	0.57	16.00	−1.20
6	−6.94	8.14E-06	0.65	32.00	−1.51
7	−7.84	1.78E-06	0.44	32.00	−1.51
8	−5.55	8.58E-05	1.24	4.00	−0.60
9	−6.43	1.94E-05	0.45	8.00	−0.90
10	−3.96	1.20E-03	0.77	4.00	−0.60
11	−4.99	2.20E-04	0.61	16.00	−1.20
12	−6.42	1.95E-05	0.45	64.00	−1.81
13	−8.49	5.97E-07	0.68	64.00	−1.81
14	−4.62	4.08E-04	0.78	8.00 [a]	−0.90
15	−6.03	3.83E-05	0.51	16.00	−1.20

[a] No definitive value was available and only the upper limit of the inhibitory potency was considered

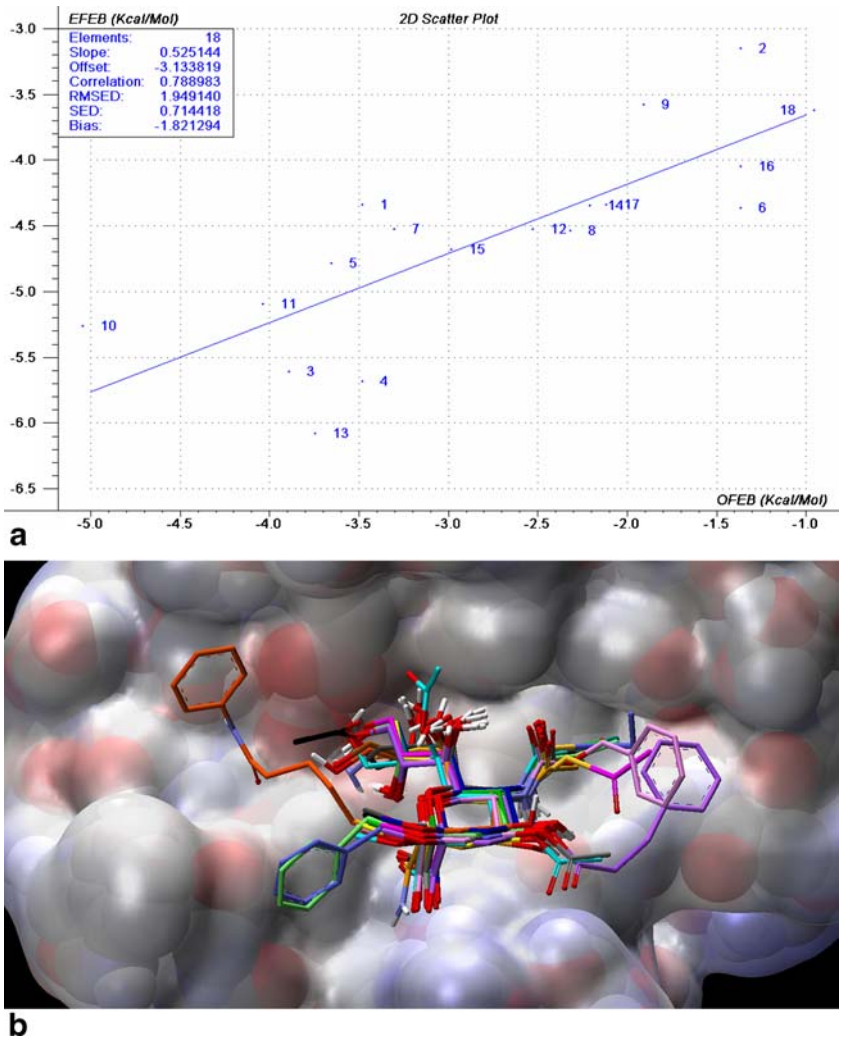

Fig. 5 Docking results for group 3 SA analogues. **a** Regression analysis showing the correlation between EFEB values calculated by AutoDock3.05 and values of the experimentally observed free energy of binding (OFEB) for all SA analogues listed in Table 3. *Y* Affinity. **b** Docked conformations of SA analogues

Table 3 Computational values for group-3 of SA analogues. Definitions as in Table 1. The observed values include dissociation constants determined by NMR experiments and the corresponding observed free energy of binding (OFEB)

Analogue no.	Computational values			Observed values	
	EFEB (kcal/mol)	K_i (mol)	RMSD of pyranose Å	K_d (mM)	OFEB (kcal/mol)
1	−4.34	6.62E-04	0.52	2.8	−3.48
2	−3.15	4.93E-03	0.71	100 [a]	−1.36
3	−5.61	7.73E-05	0.55	1.4	−3.89
4	−5.68	6.84E-05	0.59	2.8	−3.48
5	−4.79	3.10E-04	0.37	2.1	−3.65
6	−4.36	6.32E-04	0.53	100 [a]	−1.36
7	−4.53	4.82E-04	0.53	3.8	−3.30
8	−4.53	4.76E-04	0.43	20 [a]	−2.32
9	−3.58	2.39E-03	0.74	40 [a]	−1.91
10	−5.26	1.40E-04	0.58	0.20	−5.05
11	−5.09	1.85E-04	0.35	1.10	−4.04
12	−4.53	4.82E-04	0.33	14.00	−2.53
13	−6.08	3.52E-05	0.60	1.80	−3.74
14	−4.35	6.52E-04	0.54	24.00	−2.21
15	−4.68	3.72E-04	0.62	6.50	−2.98
16	−4.05	1.08E-03	0.66	100 [a]	−1.36
17	−4.34	6.62E-04	0.67	28	−2.12
18	−3.62	2.23E-03	1.82	200 [a]	−0.95

[a] No definitive value was available and only the lower limit of K_d was considered

correlation line. To further support this suggestion, correlation coefficients between group 2 and 3 inhibitors were compared. A coefficient constant for group 2 compounds constructed using $-\log(IC_{50})$ had a value similar to that of group 3 compounds, even though a stronger linear correlation between OFEB/EFEB than $-\log(IC_{50})$/EFEB is expected [26].

Root mean square error of deviations (RMSED), which is equivalent to the residual standard error, was used to measure how well the predicted and measured binding energies fitted within the model. A lower RMSED of about 2 kcal mol^{-1} was obtained for group- 3 SA analogue according to linear regression analysis established between the values of EFEB and OFEB. For group 3, the error in energy estimation was similar to the error obtained with the AutoDock3.05 calibration set (2.177 kcal mol^{-1}). However, the correlation obtained with group 3 SA analogues (r=0.79 or r^2=0.62) was lower than the correlation in the calibration set of AutoDock3.05 (r^2=0.96). This was attributed to our use of a small set of SA analogues that differ by less than two orders of magnitude in experimental affinities, compared to the greater than eight orders of magnitude difference for the AutoDock3.05 calibration set [19].

Although acceptable correlation coefficients were obtained between measured and estimated affinities, the variance values were relatively high. The measured affinities for many of the SA analogues used in this study are not definitely specified in the literature and have been recorded as ranges, which clearly affects the accuracy of correlation upon assigning a single value in the regression analysis. However, due to the limited availability of experimental compounds in the literature, these compounds were included in the experiment. The range value approach has also been used previously to construct experimental and calculated affinities [20].

Conclusions

Although the observed affinities of the majority of SA analogues used in this study differ by less than two orders of magnitude, acceptable correlations with the estimated binding energies were obtained. In other words, the scoring function of the software is able to differentiate between analogues of different affinities even though only a small window of the energy landscape is being explored.

As the presence of the central pyranose ring was the common feature in all the studied SA analogues, it was used to monitor displacement from the crystal position of methyl-α-Neu5Ac. Most of the docked SA analogues bound HA1 with a pyranose conformation close to that of the crystal methyl-α-Neu5Ac (RMSD less than 3 Å), which is consistent with the crystallographic results obtained for different SA analogues that bind to HA1 [11].

The LGA search algorithm and the semi-empirical scoring function implemented in AutoDock3.05 were able to predict the crystal position, orientation, and conformation of methyl-α-Neu5Ac with RMSD of 0.80 Å, which is better than the

currently acceptable values of less than 2 Å [25, 27, 28]. Thus, the software has good predictive power for intermolecular interactions between SA analogues and the HA1 binding pocket even though receptor flexibility is not accounted for in the calculations. The software can be used in virtual screening for searching for active SA analogues, although further improvements in the energy coefficients and the inclusion of receptor flexibility are recommended.

Recommendations

A larger training set of SA analogues with accurately determined affinities (or preferably K_d values) toward the HA1 binding pocket is required from which to derive coefficients for the energy terms of the AutoDcok3.05 scoring function, which could be used strictly for virtual screening of SA analogues.

Acknowledgment Mr. Al-qattan appreciates Universiti Sains Malaysia for supporting this project through a research fellowship scheme.

References

1. Fouchier RAM, Munster V, Wallensten A, Bestebroer TM, Herfst S, Smith D, Rimmelzwaan GF, Olsen B, Osterhaus ADME (2005) Characterization of a novel influenza a virus hemagglutinin subtype (H16) obtained from black-headed gulls. J Virol 79:2814–2882
2. Baker AT, Varghese JN, Laver WG, Colman PM (1987) Three-dimensional structure of neuraminidase of subtype N9 from an avian influenza virus. Proteins 2:111–117
3. Skehel JJ, Wiley DC (2000) Receptor binding and membrane fusion in virus entry: the influenza hemagglutinin. Annu Rev Biochem 69:531–569
4. Air GM, Laver WG (1989) The neuraminidase of influenza virus. Proteins Struc Funct Genet 6:341–356
5. Wagner R, Matrosovich M, Klenk HD (2002) Functional balance between haemagglutinin and neuraminidase in influenza virus infections. Rev Med Virol 12:159–166
6. Varki NM, Varki A (2007) Diversity in cell surface sialic acid presentations: implications for biology and disease. Lab Invest 87:851–857
7. Matrosovich M, Klenk H-D (2003) Natural and synthetic sialic acid-containing inhibitors of influenza virus receptor binding. Rev Med Virol 13:85–97
8. Carlescu I, Scutaru D, Popa M, Uglea CV (2009) Synthetic sialic-acid-containing polyvalent antiviral inhibitors. Med Chem Res 18:477–494
9. Hurt AC, Ernest J, Deng Y-M, Iannello P, Besselaar TG, Birch C, Buchy P, Chittaganpitch M, Chiu S-C, Dwyer D, Guigon A, Harrower B, Kei IP, Kok T, Lin C, McPhie K, Mohd A, Olveda R, Panayotou T, Rawlinson W et al (2009) Emergence and spread of oseltamivir-resistant A(H1N1) influenza viruses in Oceania, South East Asia and South Africa. Antivir Res 83:90–93
10. Weis W, Brown JH, Cusack S, Paulson JC, Skehel JJ, Wiley DC (1988) Structure of the influenza virus hemagglutinin complexed with its receptor sialic acid. Nature 333:426–431
11. Sauter NK, Hanson JE, Glick GD, Brown JH, Crowther RL, Park SJ, Skehel JJ, Wiley DC (1992) Binding of influenza virus hemagglutinin to analogs of its cell-surface receptor, sialic acid: analysis by proton nuclear magnetic resonance spectroscopy and X-ray crystallography. Biochemistry 31:9609–9621
12. Sauter NK, Bednarski MD, Wurzburg BA, Hanson JE, Whitesides GM, Skehel JJ, Wiley DC (1989) Hemagglutinins from two influenza virus variants bind to sialic acid derivatives with millimolar dissociation constants: a 500 MHz proton nuclear magnetic resonance study. Biochemistry 28:8388–8396
13. Machytka D, Kharitonenkov I, Isecke R, Hetterich P, Brossmer R, Klein RA, Klenk HD, Egge H (1993) Methyl alpha-glycoside of N-thioacetyl-D-neuraminic acid: a potential inhibitor of influenza A virus. A 1H NMR study. FEBS Lett 334:117–120
14. Hanson JE, Sauter NK, Skehel JJ, Wiley DC (1992) Proton nuclear magnetic resonance studies of the binding of sialosides to intact influenza virus. Virology 189:525–533
15. Pritchett TJ (1987) Receptor analogue inhibitors of influenza virus adsorption and infection. PhD thesis, University of California, Los Angeles
16. Klem S, Paulson JC, Rose U, Brossmer R, Schmid W, Bandgar BP, Schreiner E, Hartmann M, Zbiral E (1992) Use of sialic acid analogues to define functional groups involved in binding to the influenza virus hemagglutinin. Eur J Biochem 205:147–153
17. Toogood PL, Galliker PK, Glick GD, Knowles JR (1991) Monovalent sialosides that bind tightly to influenza A virus. J Med Chem 34:3138–3140
18. Al-Qattan MN, Mordi MN (2009) Site-directed fragment-based generation of virtual sialic acid databases against influenza A hemagglutinin. J Mol Model (in press) online first: doi:10.1007/s00894-009-0606-y
19. Morris GM, Goodsell DS, Halliday RS, Huey R, Hart WE, Belew RK, Olson AJ (1998) Automated docking using a Lamarckian genetic algorithm and empirical binding free energy function. J Comput Chem 19:1639–1662
20. Olsen L, Pettersson I, Hemmingsen L, Adolph H-W, Jorgenson FS (2004) Docking and scoring of metallo-β-lactamases inhibitors. J Comput Aided Mol Des 18:287–302
21. Bellocchi D, Macchiarulo A, Costantino G, Pellicciari R (2005) Docking studies on PARP-1 inhibitors: insights into the role of a binding pocket water molecule. Bioorg Med Chem 13:1151–1157
22. Hu X, Stebbins CE (2005) Molecular docking and 3D-QSAR studies of Yersinia protein tyrosine phosphate YopH inhibitors. Bioorg Med Chem 13:1101–1109
23. Zheng M, Yu K, Liu H, Luo X, Chen K, Zhu W, Jiang H (2006) QSAR analyses on avian influenza virus neuraminidase inhibitors using CoMFA, CoMSIA, and HQSAR. J Comput Aided Mol Des 20:549–566
24. Davis AM, Teague SJ, Kleywegt GJ (2003) Application and limitations of X-ray crystallographic data in structure-based ligand and drug design. Angew Chem Int Ed 42:2718–2736
25. Huey R, Morris GM, Olson AJ, Goodsell DS (2007) A semiempirical free energy force field with charge-based desolvation. J Comput Chem 28:1145–1152
26. Pearlman DA, Charifson PS (2001) Are free energy calculations useful in practice? A comparison with rapid scoring functions for the p38 MAP kinase protein system. J Med Chem 44:3417–1152
27. Ewing TJA, Makino S, Skillman AG, Kuntz ID (2001) DOCK 4.0: search strategies for automated molecular docking of flexible molecule databases. J Comput Aided Mol Des 15:411–428
28. Hanessian S, Moitessier N, Therrien E (2001) A comparative docking study and the design of potentially selective MMP inhibitors. J Comput Aided Mol Des 15:873–881